Deterioration of air quality across Sweden due to transboundary agricultural burning emissions

Admir C. Targino[1], Patricia Krecl[2], Christer Johansson[2], Erik Swietlicki[3], Andreas Massling[4], Guilherme C. Coraiola[1] and Heikki Lihavainen[5]

[1] Federal Technological University of Paraná, Av. dos Pioneiros 3131, 86036-370, Londrina, Brazil
[2] Department of Applied Environmental Sciences, Stockholm University, Svante Arrhenius väg 8, SE-114 18 Stockholm, Sweden
[3] Division of Nuclear Physics, Lund University, Professorsgatan 1, SE-221 00 Lund, Sweden
[4] Department of Atmospheric Environment, Aarhus University, Frederiksborgvej 399, DK-4000, Roskilde, Denmark
[5] Finnish Meteorological Institute, Erik Palménin aukio 1, FI-00101 Helsinki, Finland

We analyzed measurements of aerosol and trace-gas concentrations from sites across Sweden before and during a series of agricultural wildland fires in eastern Europe in spring 2006. During the burning episodes, concentrations of background particulate matter (PM) and trace gases, such as carbon monoxide and ozone, increased, affecting air quality across the country and violating national air quality standards. The European Union PM_{10} daily limit value of 50 μg m^{-3} was exceeded during the pollution episodes even at the background stations, resulting in a nearly four-fold increase as compared with that in non-episode conditions. In relation to a non-episode period, the concentration rise in the accumulation-mode particles was from 40% at an urban site to 340% at a rural site, causing an increase in total particle number concentrations. The fires also boosted ground-level ozone, increasing concentrations of this pollutant by up to 100% at the background stations, which exceeded national air quality standards. Both elemental (EC) and organic carbon (OC) levels increased, with OC making a larger contribution to the total carbonaceous concentrations during the biomass burning episodes. The large-scale atmospheric circulation determined the strength and timing of the pollution events, with the eastern and northern sectors of Sweden experiencing two pollution pulses, whilst sites in the western and southern sectors were affected by one shorter episode. The results show that regional air quality deteriorated due to the long-range transport of pollutants emitted during agricultural wildfires.

Introduction

Populations living in or around urban conglomerates are usually exposed to increased concentrations of air pollutants as a result of anthropogenic activities. Even though many countries adopted regulations to control the amount of certain pollutants discharged to the atmosphere,

such as particulate matter smaller than 2.5 and 10 micrometers in diameter ($PM_{2.5}$ and PM_{10}, respectively), ozone precursors, sulphur dioxide, and nitrogen oxides, violations of the established limit values are often observed, especially in large conurbations. For example, due to high traffic emissions, nitrogen dioxide (NO_2) and PM_{10} mass concentrations still exceed the air quality standards in Stockholm (Sweden) (Johansson *et al.* 2009). Putaud *et al.* (2010) showed that annual and daily PM_{10} limit values (40 and 50 μg m^{-3}, respectively) are exceeded in the European Union (EU) generally at (but not limited to) urban and kerbside sites, with urban background PM_{10} annual mean and median values significantly larger in southern Europe than in northwestern and central Europe. The 2010 EU target value for annual $PM_{2.5}$ mean concentration (25 μg m^{-3}) is also exceeded both at urban background and kerbside sites, as shown by the same study.

The effects of enhanced particulate matter concentration in the atmosphere were studied extensively, as they are recognized to affect the Earth's climate through absorbing and scattering solar radiation (Haywood and Boucher 2000), and aerosol particles can act as sites upon which water vapour condenses to form cloud droplets and ice crystals (e.g., Kaufmann *et al.* 2002). Aerosol particles originating from biomass burning received special attention due to their deleterious effects on human health (Lighty *et al.* 2000, Boman *et al.* 2003). Typically, smoke particle mass is predominantly in the accumulation mode (80%), whereas the coarse mode (diameter range 2.5–15 μm) accounts for 10% of the mass (Reid *et al.* 2005). In terms of particle number, count median diameters for fresh smoke are in the 0.10–0.16 μm range.

Biomass burning particles can be deposited in the human airways, and act as excellent delivery systems for aero-allergens as pollen grains and spores adhere to them and may then reach the lower respiratory tract (Löndahl *et al.* 2008). Adverse health effects have been associated with both short- and long-term exposures to particulate matter (WHO 2006). The large American Cancer Society cohort study (Pope *et al.* 2002) showed a 6% mortality increase for each 10 μg m^{-3} increase in $PM_{2.5}$ exposure. This study

was used by Forsberg *et al.* (2005) to assess the number of premature deaths in Sweden. They estimated a life-span reduction of up to seven months for the Swedish population due to the exposure to long-range transported atmospheric particles.

In addition to local pollution sources, some urban areas can be subject to pollution outbreaks caused by transboundary transport. Transboundary is a term that describes dispersion situations in which airborne contaminants cross geopolitical boundaries or migrate across several geographic zones. Biomass fires are amongst the most common transboundary pollution agents (other types include internal combustion engine emissions, power plants, etc.) According to the European Institute for Environment and Sustainability (IES), in the five southern countries (Portugal, Spain, France, Italy and Greece) about 13 000 000 ha were burnt between 1980 and 2006 (JRC-IES 2007). Combustion of agricultural crop residues by prescribed burning is another example. This is a common practice in Russia and other eastern European countries (Sillanpää *et al.* 2005, Ulevicius *et al.* 2010), and was occasionally accounted for the increase in particulate matter concentrations in western Europe (Damoah *et al.* 2004, Niemi *et al.* 2004, 2005).

When the smoke spews into the atmosphere, the population living around the fire loci is the first to suffer the consequences of higher exposure concentrations. However, the problem escalates as the smoke is transported and reaches more populated areas. Whilst local air pollution events may, to some extent, be abated by the adoption of stringent control actions, transboundary pollution events are difficult to mitigate as they may linger for a long period especially under stagnant atmospheric conditions, challenging local air pollution authorities. Another aggravating aspect is that transboundary pollution may be emitted by countries in which this form of emission is not regulated. In such situation, little or no coercive measure can be adopted against the nation in which the uncontrolled emissions occurred.

In spring 2006, the burning of agricultural crop residues become uncontrolled in Belarus, Baltic countries, the Ukraine and western Russia and the developed wildfires covered a vast area

(~20 000 km²) (Stohl *et al.* 2007). The transport of the smoke plumes from the wildfire areas lasted for about 12 days and — sparked by a severe heat wave, drought and favourable large-scale circulation — the polluted plume was carried to regions as far as the Arctic (Stohl *et al.* 2007, Treffeinsen *et al.* 2007), spanning northern Europe (Saarikoski *et al.* 2007, Sopauskiene and Jasineviciene 2009) and the United Kingdom (Witham and Manning 2007), causing severe air quality deterioration.

The purpose of this study was to assess the impact of the transboundary agricultural burning event of spring 2006 on the air quality at sites across Sweden. We looked particularly at PM_{10} and $PM_{2.5}$ mass concentrations, carbonaceous aerosol content, particle number size distributions, as well as key trace gases, such as ozone (O_3) and carbon monoxide (CO).

Experimental methods

Sampling sites

In this work, we analyzed measurements from several monitoring sites installed in Stockholm (Essingeleden, Hornsgatan, Norrlandsgatan, Sveavägen, and Torkel managed by the Stockholm Environment and Health Administration), Uppsala, Gothenburg (Femman and Gårda) and Malmö (Fig. 1 and Table 1).

The Essingeleden site is located at the kerb-side of the eight-lane E4 motorway (128 000 vehicles/day) on the Lilla Essingen island, in southern Stockholm. The Hornsgatan station is located in a 24-m-wide four-lane street canyon (35 000 vehicles/day) in the Stockholm city centre. Air intakes are placed on both sides of the street at 3-m height (about 1.5 m from the façades), and also on the roof of a building some 500 m east of Hornsgatan, in an area with less traffic. The roof measurements represent the urban background in Stockholm. The Norrlandsgatan station is located in the Stockholm centre, on a 15-m-wide two-lane one-way street (10 000 vehicles/day) surrounded on both sides by 24-m-high buildings. Measurements are conducted 2 m above the street level and represent a traffic-impacted environment. The Sveavägen
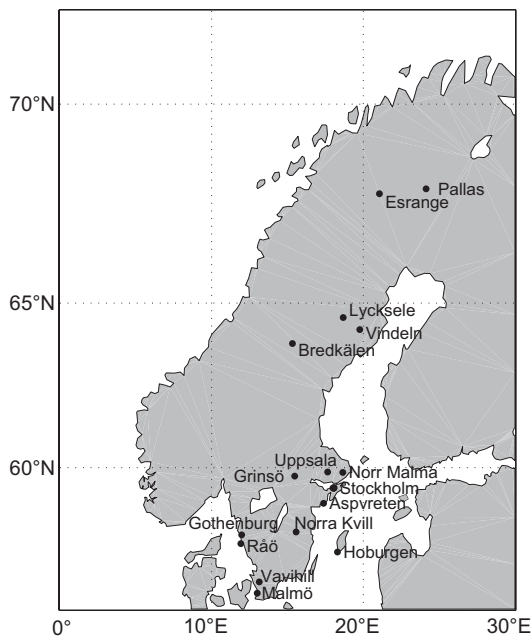
Fig. 1. Locations of the stations considered in this study. Due to the short distance between them, the Stockholm urban stations — Essingeleden, Hornsgatan, Norrlandsgatan, Sveavägen, and Torkel — are not shown separately.

station is situated in central Stockholm, on a 33-m wide four-lane street (30 000 vehicles/day) surrounded on both sides by 20-m-high houses. Measurements are carried out 2 m above the street level and represent a traffic-impacted environment. The Torkel station is located at the rooftop level (25 m high), and thereby represents urban background concentrations for the Stockholm region.

The Uppsala site is a kerbside station in Kungsgatan (18 000 vehicles/day) in central Uppsala. Femman is an urban background site located on a rooftop (30 m high) in central Gothenburg and close to the harbour. Gårda is placed by the kerbside of the four-lane E6 motorway (79 000 vehicles/day) in Gothenburg. The Malmö site is an urban background station installed on the rooftop of the city Town Hall, in the town's inner core on the south coast of Sweden. Malmö is the largest city in the Scania province of southern Sweden with relatively high pollutant concentrations due to busy motorways, several busy harbours and the proximity to Copenhagen and to continental Europe.

Measurements conducted at the following rural background stations were also analyzed: Aspvreten, Bredkälen, Esrange, Grimsö, Hoburg, Norr Malma, Norra Kvill, Råö, Vavihill, and Vindeln (Table 1). All of them, except for Norr Malma (operated by the Stockholm Environment and Health Administration), are a part of the European Monitoring and Evaluating Programme (EMEP). Aspvreten and Vavihill are also a part of the European Supersites for Atmospheric Aerosol Research (EUSAAR) network. The Aspvreten site is about 80 km southwest of Stockholm and 2 km west of the Baltic coast and it is surrounded by mixed coniferous and deciduous forests (Tunved et al. 2003). Bredkälen is located in the northern lowland areas of Sweden and surrounded by coniferous forest, grasslands and pasture. The Esrange station is located in the northern part of Sweden, in a low and sparse coniferous forest, on a hill top at 475 m a.s.l. and 170 m above the surrounding landscape. Grimsö is located in central Sweden and has a low posi-

tion in the local forest landscape. Hoburg is situated on the southern coast of the Island of Gotland (Baltic Sea), and it is surrounded by grassland and farmland. Norr Malma is an inland station located 70 km north-east of Stockholm and 1 km south of lake Erken. Norra Kvill is located in southeast Sweden and is positioned very high in the local landscape (250 m a.s.l.). The Råö station is situated on the southwest Swedish coast, with nearby areas covered by low vegetation, and bare cliffs and open sea to the west. The Vavihill station, operated by the Lund University, is located in southern Sweden, in a small meadow near a ridge top largely covered by deciduous and coniferous forests with no influence from local pollution sources. Vindeln is in the middle boreal zone surrounded by mature coniferous forests about 190 km south of the Arctic Circle and positioned at 225 m a.s.l. in the lower part of a long slope facing southward.

Measurements conducted at the Finnish Pallas station (main site at Sammaltunturi) were

Table 1. Summary of sites and measurements used in this study. K = kerbside, RB = rural background, U = urban, and UB = urban background.

Sites	Type	Gases			Aerosols					
		O_3	CO	NO_x	PM_{10}	$PM_{2.5}$	Size distribution	EC/OC	BS	LAC
Aspvreten	RB	x			x		x	x		x
Bredkälen	RB			x[a]					x	
Esrange	RB	x								
Stockholm(Essingeleden)	K			x	x	x				x
Gothenburg (Femman)	UB				x					
Gothenburg (Gårda)	K				x					
Grimsö	RB	x								
Hoburg	RB								x	
Stockholm (Hornsgatan)	K		x	x	x		x			x
Stockholm (Hornsgatan)	UB		x	x						
Malmö	UB	x		x			x			
Norra Kvill	RB	x								
Stockholm(Norrlandsgatan)	U			x	x	x				
Norr Malma	RB	x		x[a]	x	x				
Pallas	RB	x					x			
Råö	RB	x		x[a]	x				x	
Stockholm (Sveavägen)	U		x		x					
Stockholm (Sveavägen)	UB		x							
Stockholm (Torkel)	UB	x		x	x	x		x		x
Uppsala	K				x	x				
Vavihill	RB	x		x	x	x	x		x	
Vindeln	RB	x			x					

[a] Only NO_2 measurements.

also included to increase the data coverage in the northern region. Due to its proximity to the Finnish–Swedish border (~30 km), the data were considered representative of the air quality of northern Sweden. Sammaltunturi is located on a hill top (560 m a.s.l) in the boreal forest zone, with no large local or regional pollution sources. The station is a part of the Global Atmosphere Watch (GAW) programme and is run by the Finnish Meteorological Institute.

Measurements

Aerosol mass concentration

The mass concentrations of PM_{10} and $PM_{2.5}$ were measured using Tapered Element Oscillating Microbalances (TEOM© 14001, Rupprecht & Patashnick Inc., USA) with heated inlets (50 °C) to avoid condensation of water. To account for losses of volatile material, all TEOM data were corrected following Areskoug (2007). In short, built-in TEOM corrections were removed, mass concentrations were expressed at ambient pressure and temperature and, finally, concentrations were multiplied by 1.19 and an offset of 1.15 was added. Daily averages were calculated from 1-h average resolution data.

Particle number size distribution

The particle number size distribution was measured with a differential mobility particle sizer (DMPS). DMPS systems consist of a particle charger and a differential mobility analyser (DMA) coupled with a condensation particle counter (CPC). The system classifies the charged particles into size ranges according to their electrical mobility. The different size bins are separated by changing the voltage difference inside the DMA, and the charged particles in every size division are subsequently counted by the CPC. The particle diameter ranges and scanning frequencies of each DMPS were as follows: 28–765 nm and 2 min at Hornsgatan, 3–858 nm and 10 min at Vavihill, 10–551 nm and 3 min at Malmö, 10–451 and 6 min at Aspvreten, and 7–479 nm and 10 min at Pallas. The data were averaged for 1 hour.

Carbonaceous aerosols

Measurements of aerosol light absorption coefficient, b_{ap}, were done using custom-built Particle Soot Absorption Photometers (PSAP), from which the mass concentration of light-absorbing carbon (LAC) was derived. The method is based on the integrating plate technique (Lin *et al*. 1973) that measures the attenuation of light transmitted through particles that are continuously collected on a filter. The LAC mass absorption cross section, σ_{abs}, relates the absorption coefficient of the aerosol to the LAC mass concentration, M_{LAC}. To convert b_{ap} into M_{LAC}, a site- and season-dependent σ_{abs} value of 10.0 $m^2 g^{-1}$ was used for Aspvreten, and 7.6 $m^2 g^{-1}$ for Torkel, Hornsgatan and Essigeleden, as determined by Krecl *et al*. (2011).

Daily black smoke (BS) measurements were conducted at some EMEP background sites. In short, particle-laden air was sampled through a filter and the darkness of the stain was measured by optical reflectance and converted to a black smoke index (expressed as $\mu g\ m^{-3}$) using a standard table. Airborne particles were collected on a Whatman 1 paper filter through a sample inlet, equipped with an inverted funnel, using a semi-automatic low-volume sampler. Sampling of particles, reflectance measurements, and calculation of BS index were done according to specifications of the SS-ISO 9835, which is the Swedish version of the international standard ISO 9835 (1993).

For elemental carbon (EC) and organic carbon (OC) analyses, quartz fibre filters were collected at Torkel and Aspvreten using a 10-μm cut-off size sequential sampler installed at a height of 1.6 m above the rooftop level and operated at a standard flow rate of 38.3 l min^{-1}. Filters were pre-baked in a furnace at 800 °C for 150 minutes and placed in clean glass Petri dishes and kept refrigerated before and after the filter sampling. The EC/OC analysis of 1.5 cm^2 rectangular filter punches was carried out using a Thermal/Optical Carbon Aerosol Analyzer (Sunset Laboratory Inc., Forest Grove, USA) operated according to the NIOSH method 5040 (Birch and Cary 1996). A total of 45 field filters were analysed for Torkel (28 samples exposed 12-h, 14 daily filters, and 3 blank filters), whereas five weekly exposed filters and one blank filter were analysed for
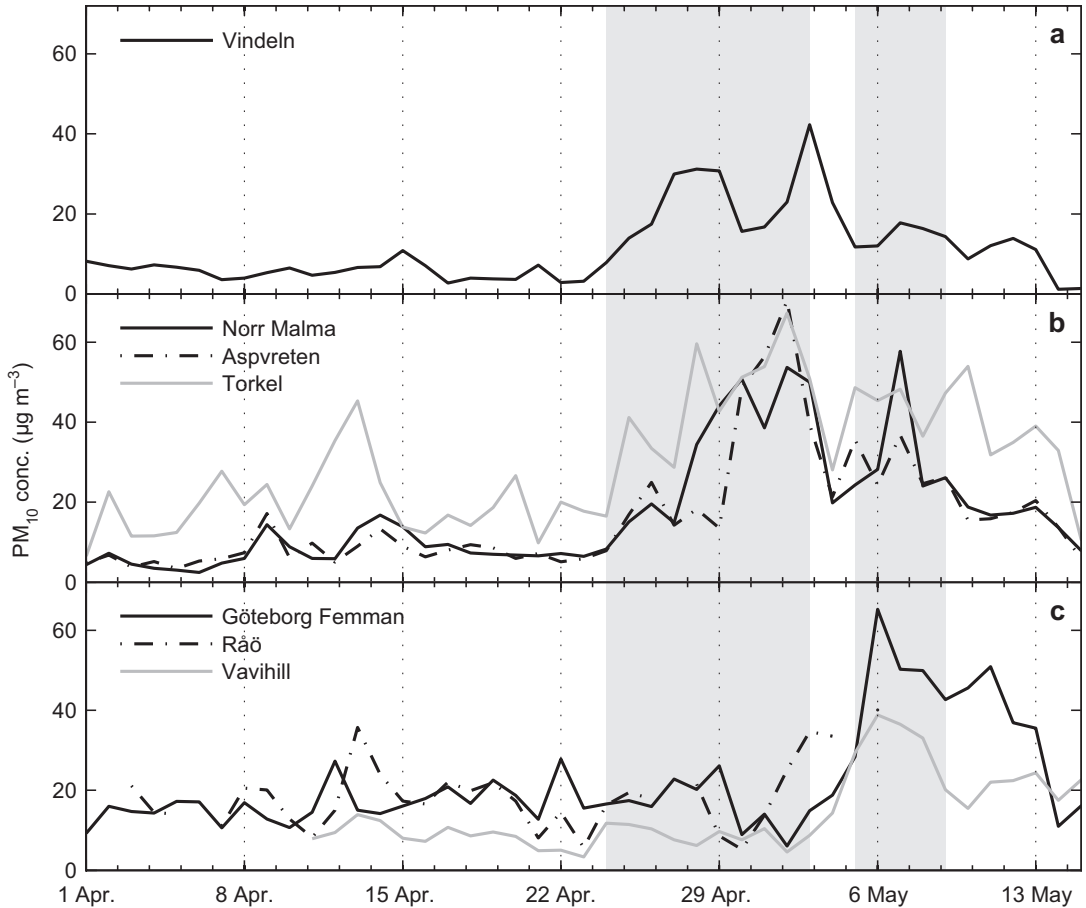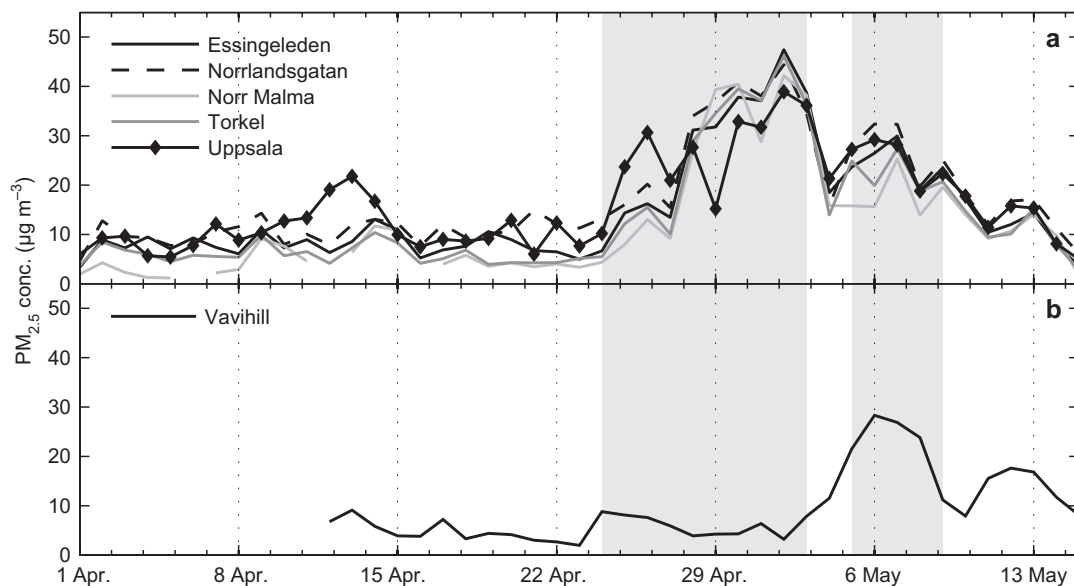
Fig. 2. Daily mean PM$_{10}$ mass concentrations at the background stations across Sweden: (**a**) northern Sweden, (**b**) Stockholm area, (**c**) southern Sweden. The shaded areas delimit POLL1 and POLL2 episodes.

Aspvreten. The final OC mass concentration was calculated by subtracting the concentration of the corresponding blank filter from the OC fraction. The OC baseline represented 18% and 4% of the amount analysed on ambient samples collected in the REF and polluted periods, respectively, whereas the field blanks for EC were zero. However, OC mass concentrations could be still overestimated after using this simple correction. Negative artefacts due to evaporation of semivolatile particulate matter from the sampled filter were not quantified in this work.

Trace gas measurements

Concentrations of CO were measured using automatic infrared-absorption CO analysers

(Thermo Scientific, model 48i with Ndir technology) and 15-min averages were logged. Ozone measurements were carried out continuously by UV-absorption ozone monitors. EMEP stations were equipped with Monitor Lab instruments (model ML9810, USA) with inlet heights at about 4–5 m above ground, and hourly averages were recorded. Ozone concentrations at the Torkel and Norr Malma sites were monitored by analysers manufactured by Environment S.A. (France, model 42M), and 15-min averages were logged. NO$_x$ measurements were conducted with chemiluminiscence analyzers (Environment SA, mod 31 M LCD) and 15-min averages were logged. Daily NO$_2$ measurements at EMEP sites were obtained by NaI-impregnated glass sinters (flow rate of ~0.7 m^3/day) and spectrophotometric flow injection analysis.

Fig. 3. Daily mean $PM_{2.5}$ mass concentrations at the stations across Sweden: (**a**) Stockholm area, (**b**) southern Sweden. The shaded areas delimit POLL1 and POLL2 episodes.

Results and discussion

Aerosol mass concentration

In Sweden, the wildfire pollution episode was first observed on 24 April 2006 at the stations in and around Stockholm. The signal was more clearly discernible at the background stations such as Norr Malma, Aspvreten and Torkel (*see* the PM_{10} concentration time series in Fig. 2b). Moreover, the urban kerbside stations, such as Norrlandsgatan and Essingenleden in Stockholm, also registered prominent $PM_{2.5}$ peaks, with abnormally elevated levels as high as 40 μg m^{-3} (Fig. 3a). In this study, three periods were highlighted (Figs. 2 and 3): reference (REF: 1–23 April), and two pollution periods coincident with the wildfire outbreaks (POLL1: 24 April–3 May and POLL2: 5–9 May). The pollution periods were separated by a relatively cleaner period during which $PM_{2.5}$ and PM_{10} concentrations decreased at the urban background stations around Stockholm. This period was not affected by long-range pollution advection, as determined by inspection of five-day air mass trajectories calculated with the HYSPLIT model (Draxler and Rolph 2011) using the reanalysis

(global, 1948–present) database. The trajectories were calculated once per day, arriving at 00 UTC at heights of 500, 1000 and 1500 m above the ground level.

The atmospheric general circulation over Europe in late April and early May was governed by the Iceland low pressure system and a quasi-stationary anticyclone centred over Russia (Stohl *et al.* 2007, Treffeisen *et al.* 2007). This synoptic situation facilitated the channelling of air between these two systems along a south–north axis. From 29 April to 2 May, the western side of the anticyclone was positioned over northern Scandinavia and the air from the fire area was first carried west around the high pressure system and then to the north. This corresponds with the monitoring stations in southern Sweden not experiencing elevated pollution levels during the first episode (Figs. 2c and 3b). On 4 May, the anticyclone over Russia moved eastward and only a very small component of the air had originated over the fire area. This was subsequently followed by a new pulse of polluted air which reached southern Sweden and, to a lesser extent, more northerly stations of the country. The stations around Stockholm were affected by both pollution episodes with PM_{10} concen-

trations reaching values as high as 82 μg m^{-3} in Aspvreten, and 108 μg m^{-3} in Torkel. Mean values for these stations during the reference period were 7.6 and 19.9 μg m^{-3}, respectively (Table 2). Whilst the air quality at the sites in eastern Sweden (Norr Malma, Aspvreten and Torkel) was deteriorated during POLL1, PM$_{10}$ mass concentrations at the southerly sites such as Råö, Gothenburg and Vavihill were at the same level as during the reference period (Fig. 2c and Table 2). On 5 May, PM$_{10}$ concentrations in Gothenburg and Vavihill started to increase and remained above 40 μg m^{-3} until 13 May. Due to the lack of data, it is not possible to establish if PM$_{10}$ concentrations in Råö followed the same pattern. However, it was possible to observe an increase in PM$_{10}$ concentration already on 4 May.

The first pollution episode was also observed in northern Sweden with PM$_{10}$ concentration at Vindeln increasing from mean background values of 5.6 μg m^{-3} to values as high as 40.0 μg m^{-3} (Fig. 2a). Elevated levels of PM$_{2.5}$ were measured at the urban and background sites around Stockholm and in Uppsala (Fig. 3a and Table 3). In southern Sweden, PM$_{10}$ and PM$_{2.5}$ concentrations peaked contemporaneously during the second pollution episode (Figs. 2c and 3b). During spring, it is common to register high PM$_{10}$ concentrations at urban sites in Sweden. This is due to non-exhaust traffic particles arising from both abrasion of asphalt by studded tyres and resuspension of particles from the road surface (Norman and Johansson 2006).

These smoke episodes were concurrently recorded in neighbouring countries, such as Finland and Lithuania. In Finland, PM$_{2.5}$ concentrations started to increase on 25 April 2006 in Helsinki (urban background site), remaining significantly elevated for almost 12 days and reaching values as high as 70 μg m^{-3} (Saarikoski *et al.* 2007). In Lithuania, an increase in PM$_{10}$ concentrations coincident with the wildfire outbreak was recorded on 29 April 2006 reaching over 73 μg m^{-3} at an urban background station in Vilnius (Sopauskiene and Jasineviciene 2009). Critical PM$_{10}$ daily values showed a maximum of 130 μg m^{-3} on 2 May 2006 in Vilnius and remained elevated until 7 May.

Trace gas concentrations

Biomass combustion emits a variety of trace gases, among them CO and NO$_2$ (Andreae and Merlet 2001). Ozone is a secondary pollutant whose formation depends on the temperature, humidity and solar radiation as well as the primary emissions of NO$_x$ and volatile organic compounds. Under favourable dispersion conditions, the outreach of these trace gases depends on their atmospheric residence time.

Similarly to the measurements of PM$_{10}$, the stations in northern and central Sweden registered elevated O$_3$ concentrations during POLL1 and POLL2 (Fig. 4a and b), whilst at the stations in the south, a deviation from non-episode values was recorded only during the second event (Fig. 4c). O$_3$ levels at the rural background stations like Aspvreten (Fig. 4b) and Vavihill (Fig. 4c) doubled from around 70 μg m^{-3} to 150 μg m^{-3}. Measurements across the UK (Witham and Manning 2007), Finland (Anttila *et al.* 2008) and Svalbard (Stohl *et al.* 2007) demonstrated similar elevated levels of O$_3$ during the pollution outbreak, which was attributed to biomass burning in eastern Europe.

Due to the high impact of traffic emissions on kerbside CO concentrations, no LRT signal was clearly detected at the kerbside stations, hence only the rooftop measurements of CO in central Stockholm are considered (Fig. 4d). CO concentration at these urban background stations increased from 0.3 mg m^{-3} to 0.45 mg m^{-3} at Hornsgatan and 0.5 mg m^{-3} at Sveavägen.

NO$_x$ time series showed no increase during the pollution episodes, and concentrations were comparable to values during the REF period (not shown here). Witham and Manning (2007) found similar results and reported no NO$_x$ concentration increase associated with raised PM$_{10}$ levels in the UK during this pollution outbreak.

Carbonaceous aerosols

Simultaneously with PM$_{10}$ and PM$_{2.5}$ concentrations, the carbonaceous aerosol content increased during the pollution events (Fig. 5). The two episodes are recognisable in the time series of M_{LAC}

Table 2. Statistics of PM_{10} hourly averages ($\mu g\ m^{-3}$) for stations across Sweden during the reference (REF), pollution 1 (POLL 1) and pollution 2 (POLL 2) periods.

Station	Mean	SD	5th percentile	95th percentile	Max.
Vindeln					
REF	5.6	3.4	1.5	11.2	26.1
POLL 1	24.8	13.5	8.0	52.7	67.9
POLL 2	13.8	5.7	7.5	26.0	33.6
Norr Malma					
REF	7.8	5.6	1.3	19.3	31.0
POLL 1	35.6	17.0	8.3	61.4	77.3
POLL 2	31.2	26.9	13.9	102.1	161.6
Aspvreten					
REF	7.6	5.3	1.1	17.7	32.3
POLL 1	33.9	23.2	3.3	71.1	81.6
POLL 2	25.6	13.9	7.8	50.9	59.6
Stockholm (Hornsgatan)					
REF	67.0	62.3	8.4	208.1	344.6
POLL 1	86.6	51.8	35.9	191.4	407.4
POLL 2	100.0	38.1	46.2	175.5	223.5
Stockholm (Torkel)					
REF	19.9	14.1	4.8	47.1	101.8
POLL 1	47.5	19.4	13.9	77.5	107.7
POLL 2	46.3	15.8	24.7	74.0	81.5
Uppsala					
REF	47.8	55.8	5.2	151.3	483.3
POLL 1	81.5	58.7	10.4	203.3	285.7
POLL 2	60.0	27.5	26.7	109.3	181.2
Stockholm (Sveavägen)					
REF	58.9	49.4	6.9	155.2	278.9
POLL 1	69.0	38.3	27.5	131.0	315.3
POLL 2	56.4	22.0	29.1	92.7	142.5
Stockholm (Essingeleden)					
REF	72.3	58.9	8.6	190.2	309.3
POLL 1	92.0	54.5	28.8	203.6	275.2
POLL 2	89.6	49.5	44.2	182.7	392.5
Stockholm (Norrlandsgatan)					
REF	67.5	55.3	7.6	177.9	328.2
POLL 1	73.5	31.5	35.7	133.0	229.0
POLL 2	71.6	31.5	31.5	137.2	170.6
Råö[a]					
REF	16.7	6.6	7.1	28.7	35.7
POLL 1	18.1	8.8	5.2	34.7	34.7
POLL 2	–	–	–	–	–
Gothenburg (Femman)					
REF	16.8	8.4	5.9	31.1	73.2
POLL 1	16.3	11.7	4.2	33.9	88.6
POLL 2	50.6	15.9	28.8	75.2	94.0
Gothenburg (Gårda)					
REF	31.1	20.2	9.6	75.7	134.6
POLL 1	29.4	20.5	8.7	73.1	131.6
POLL 2	51.1	20.1	28.0	100.5	128.8
Vavihill					
REF	8.7	4.3	2.5	17.2	23.4
POLL 1	8.5	5.2	3.0	17.0	34.0
POLL 2	29.1	10.0	13.4	43.0	46.0

[a] Daily averages.

and BS (Fig. 5a and b, respectively) for the stations in and around Stockholm, and in southern Sweden, and EC and OC (together with PM_{10} concentration) at Aspvreten and Torkel (Fig. 5c and d, respectively).

Krecl *et al.* (2011) analysed in detail the M_{LAC} concentrations at the same sites between 20 April and 5 July 2006. Their results suggest that vehicle exhaust emissions were mainly responsible for the high M_{LAC} concentrations found at Stockholm's kerbside sites (Hornsgatan and Essingeleden), whereas the long-range transport of wildfire emissions caused a large increase of levels at the background sites (Torkel and Aspvreten). However, the street contribution to the M_{LAC} concentrations at the kerbsides in Stockholm was drastically reduced on 1 May (bank holiday) during POLL1, when a mean M_{LAC} value of ~4.0 μg m^{-3} was measured at the kerbside and urban background sites (Fig. 5a). Traffic counts were lower than usual on that day (Monday) and on the previous weekend due to the bank holiday. Thus, regional transport of combustion-derived particles became an important source of M_{LAC} on 1 May even at the kerbside stations in Stockholm.

The impact of transboundary pollution on the carbon content was higher in southern Sweden (Vavihill, Hoburg, and Råö) during the POLL2 episode with maximum BS values on 6 May, as previously commented when analyzing the PM measurements for the same area.

Whilst the OC concentration rose during the pollution episodes, the EC concentration did not increase as much (Table 4). The average OC concentration was about five times higher during POLL1 as compared with that during the REF period at Torkel, whereas the concentratios at Aspvreten was 11 times higher. EC concentrations increased about 3 fold at both sites during the pollution episodes. Note that only one filter was exposed at Aspvreten during POLL2 (1–8 May) when the OC concentration was highest. However, it is most likely that the highest OC load occurred on the first days of the sampling (1–4 May, within POLL1), as observed at the other site. During POLL2, we cannot rule out the possible contribution of pollen particles to

Table 3. Statistics of $PM_{2.5}$ hourly averages (μg m^{-3}) for stations across Sweden during the reference (REF), pollution 1 (POLL 1) and pollution 2 (POLL 2) periods.

Station	Mean	SD	5th percentile	95th percentile	Max.
Stockholm (Essingeleden)					
REF	8.0	4.5	1.9	16.5	28.3
POLL1	29.7	14.4	7.7	53.2	58.1
POLL2	23.2	9.2	8.8	37.9	46.8
Stockholm (Torkel)					
REF	6.0	3.4	1.8	12.6	21.7
POLL1	28.7	14.6	7.2	50.9	54.5
POLL2	20.4	9.2	7.7	35.9	46.0
Stockholm (Norrlandsgatan)					
REF	10.8	5.7	2.9	20.6	41.7
POLL1	30.8	13.2	11.1	50.2	55.7
POLL2	25.3	9.8	10.6	42.5	46.7
Norr Malma					
REF	4.9	4.6	0.5	14.3	25.9
POLL1	27.0	15.1	3.9	48.2	60.8
POLL2	17.8	8.7	6.6	38.5	53.4
Uppsala					
REF	10.9	7.4	3.3	24.0	62.5
POLL1	28.7	12.5	7.2	49.6	63.8
POLL2	23.3	8.8	11.0	39.6	56.5
Vavihill					
REF	5.1	3.4	1.0	12.1	16.0
POLL1	5.7	4.4	1.0	15.0	27.1
POLL2	19.6	9.2	6.4	32.0	38.0
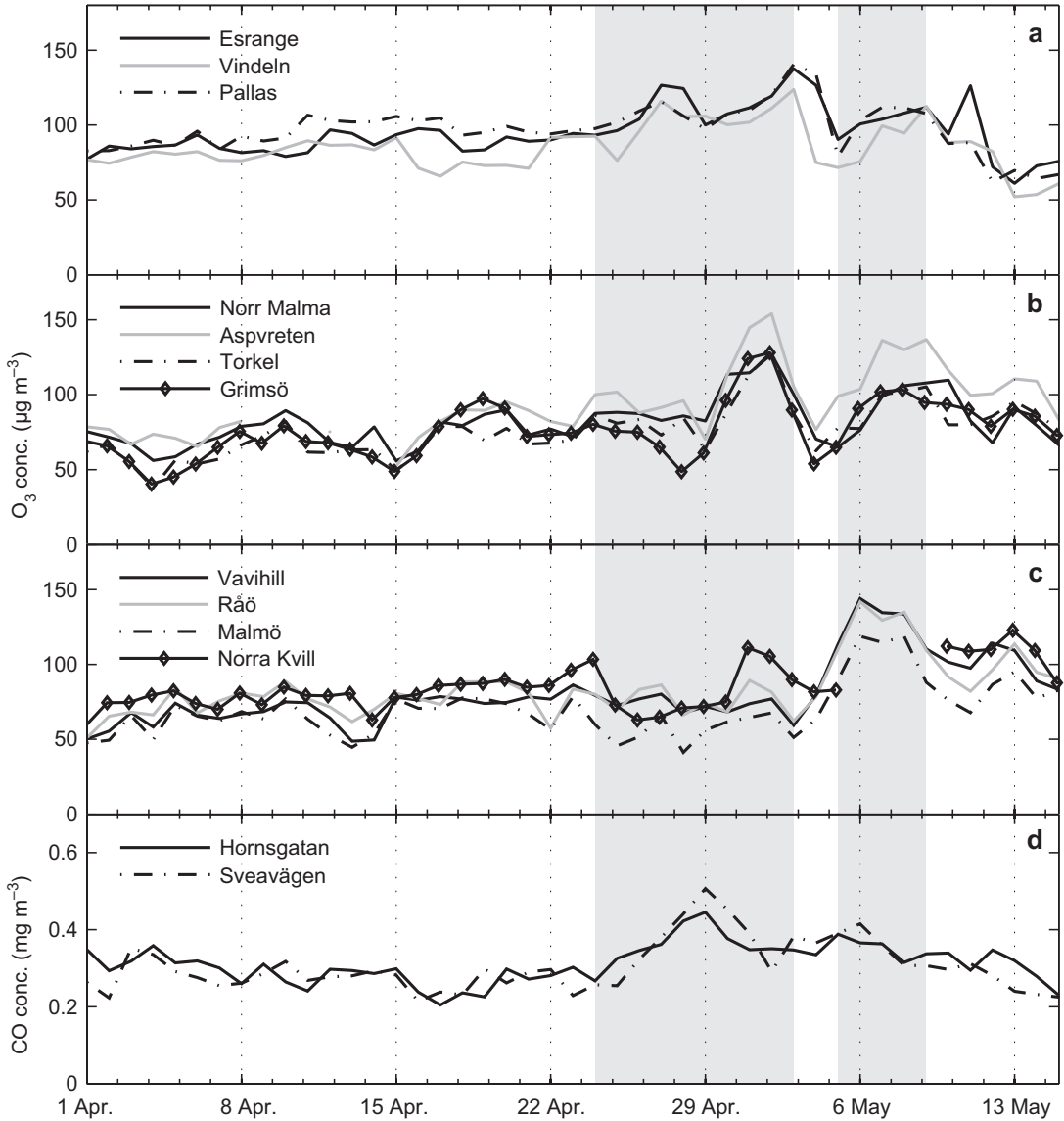
Fig. 4. Daily mean O_3 concentrations at the background stations across Sweden: (**a**) northern Sweden, (**b**) Stockholm area, (**c**) southern Sweden. (**d**) Daily mean CO concentrations measured at the background sites. The shaded areas delimit POLL1 and POLL2 episodes.

the OC concentrations, since an intense pollen outbreak (mostly birch) was observed over Scandinavia on 4–12 May 2006, with peak daily values of 4900 counts m⁻³ in Stockholm on 6 May. Even though, the EC/OC sampler at both sites was equipped with a PM_{10} cut-off device, fragmented pollen particles could have reached the collection filter. Thus, the values of OC concentrations during POLL2 should be considered with caution. The contribution of EC to the PM_{10}

load remained rather constant (~2%) at both sites over the entire sampling period, whereas the OC fraction increased from 7% to 20% at Aspvreten and from 12% to 20% at Torkel. Saarikoski *et al.* (2007) also found substantially elevated OC concentrations during both episodes investigated here as compared with those during the reference period at an urban background site in Helsinki, whereas EC concentrations increased 4 fold at the same site due to the wildfires (Table 4). The
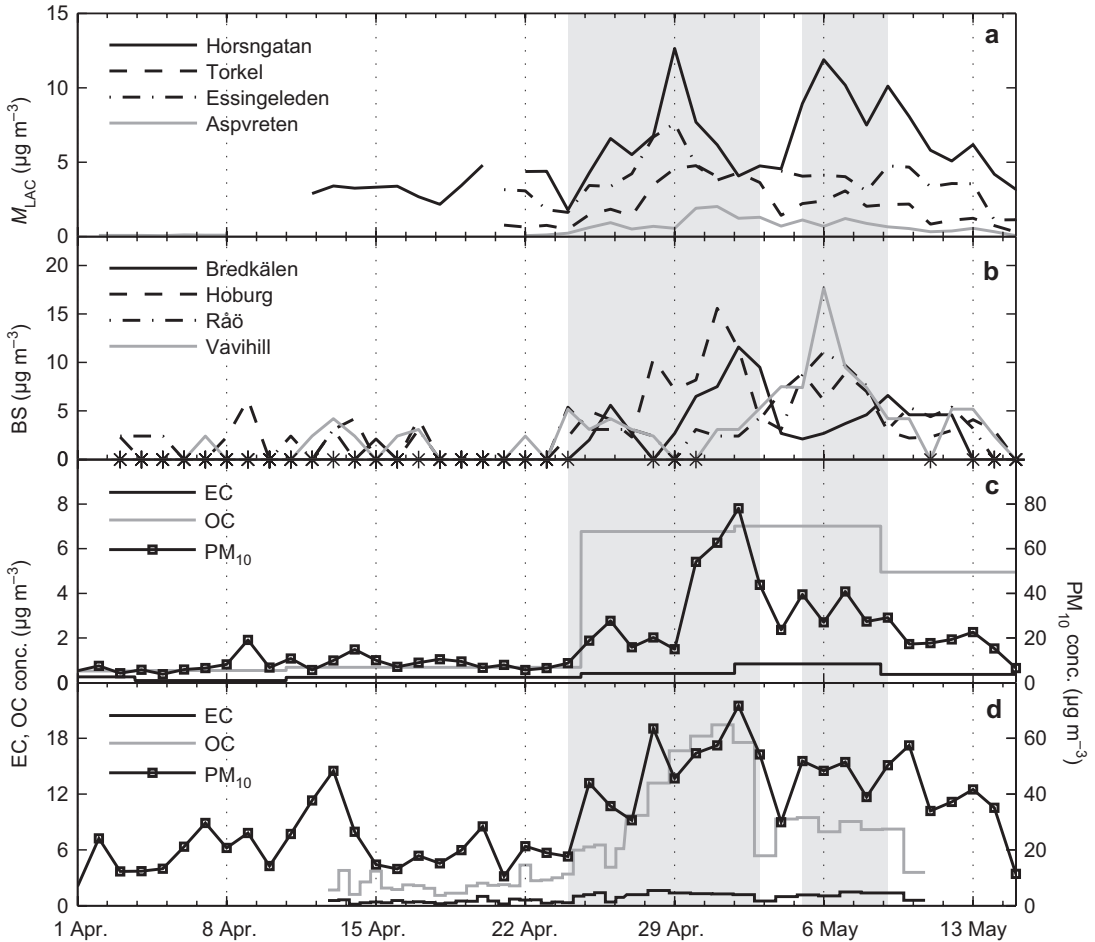
Fig. 5. (**a**) Daily mean time series of M_{LAC} in and around Stockholm, and (**b**) BS measured at the sites across Sweden. Asterisks (*) indicate BS values below the detection limit of 1.5 μg m^{-3}. Time series of EC, OC, and PM$_{10}$ for (**c**) Aspvreten and (**d**) Torkel. The shaded areas delimit POLL1 and POLL2 episodes.

decrease in OC and EC concentrations found along the plume pathways when comparing Helsinki, Stockholm and Svalbard measurements can be attributed to dilution and mixing during the long-range transport of smoke.

The EC/OC ratio is commonly used as an indicator of combustion temperature to distinguish between biomass burning and internal engines combustion. More efficient combustion produces large amounts of EC whereas inefficient combustion emits a wide range of organic compounds (Khalil and Rasmussen 2003, Frey *et al*. 2009). In Europe, urban roadside areas largely impacted by traffic emissions are characterised by high EC/OC ratios (0.44–0.77) as compared with the urban background (0.24–0.46), rural

(0.11–0.38) and remote (0.15–0.27) sites where emissions of EC are limited (Pio *et al*. 2011). Studies of fresh-biomass-burning particles in temperate and boreal regions found low EC/OC ratios (0.03–0.15), especially during smoldering conditions (Reid *et al*. 2005). The EC/OC ratios of this study were compared with values reported by Stohl *et al*. (2007) and Saarikoski *et al*. (2007) for the same events (Table 4). The large uncertainties, usually found when comparing EC and OC results determined by different analytical methods (Reid *et al*. 2005), are expected to be reduced in our comparison since the same technique (Sunset analyzers run with the NIOSH protocol) was used to analyse filters collected at different sites. Regardless of the station type

(i.e. urban background or rural), EC/OC ratios decreased at all sites during the pollution periods (minimum values for POLL1) as compared with those for the reference period. Stohl *et al.* (2007) found an EC/OC ratio of 0.06 at Svalbard in the period 30 April–7 May 2006, which is as low as the ratio observed at the Aspvreten rural site during POLL1. Despite the high complexity of emission sources at different sites and long-range transport of pollutants, these results suggest that the increase of the OC content in the aerosol carbonaceous load observed during plume events was mainly due to the transport of wildfire smoke originated in eastern Europe.

Aerosol number size distribution

The pollution outbreaks did not only affect aerosol mass concentration, but also caused a remarkable increase in total particle number concentrations and change in aerosol number size distributions. We investigated the daily time series of integrated particle number concentrations over the entire size range (N_{tot}), mean particle number concentrations for particles > 100 nm in diameter (N_{100}), along with daily mean particle number size distributions for five stations across Sweden on selected days (Fig. 6; for

the background sites, particle number concentrations for particles > 30 nm in diameter (N_{30}) are also shown).

Under unperturbed conditions (6 April 2006), the daily mean particle number size distribution at Pallas was bimodal (peaks at 40 and 250 nm), with almost equal contributions from the accumulation and Aitken modes (Fig. 6b). This distribution is in agreement with the results of Tunved *et al.* (2003) who found that the Aitken and accumulation modes were well separated with modal peaks at 50 and 210 nm in the spring months. On 20–23 April, N_{tot} increased (maximum of 200 cm^{-3} on 23 April) due to nucleation events as depicted by the N_{30} time series, whereas N_{100} remained at the background levels. Following Tunved *et al.* (2003), in this study, particles smaller than 30 nm were interpreted as nucleation mode particles. In northern Sweden, the pollution plume signal was first registered on 24 April, as shown by the increase of N_{100} at Pallas, remaining high until 3 May (Fig. 6a). On 2 and 7 May, within POLL1 and POLL2, the size distribution was characterised by the complete absence of the Aitken mode and an increase in the number of accumulation mode particles, a pattern also observed on Svalbard by Stohl *et al.* (2007). This change in mode and enhancement of particle number concentrations

Table 4. Average EC and OC concentrations, along with EC/OC ratios for several sites during reference and LRT pollution episodes in spring 2006. *n* = number of samples.

| Station	Dates	*n*	EC (μg m^{-3})	OC (μg m^{-3})	EC/OC	References
Stockholm (Torkel[a])						
REF	12–24 Apr	23	0.38	2.04	0.18	This study
POLL1	24 Apr–2 May	11	1.01	9.85	0.10	
POLL2	3–9 May	6	1.07	7.61	0.14	
Aspvreten[a]						
REF	3–24 Apr	2	0.15	0.55	0.27	This study
POLL1	24 Apr–1 May	1	0.37	6.10	0.06	
POLL2	1–8 May	1	0.76	6.31	0.12	
Svalbard[a]						
POLL1	23–30 Apr	1	0.10	0.40	0.25	Stohl *et al.* (2007)
POLL2	30 Apr–7 May	1	0.24	3.60	0.06	
Helsinki[b]						
REF	24 Mar–24 Apr	19	0.59	1.30	0.45	Saarikoski *et al.* (2007)
POLL1	24–29 Apr	8	2.40	11.00	0.22	
POLL2	1–5 May	8	2.50	9.70	0.25	

[a] PM$_{10}$ cut-off size, [b] PM$_1$ cut-off size.
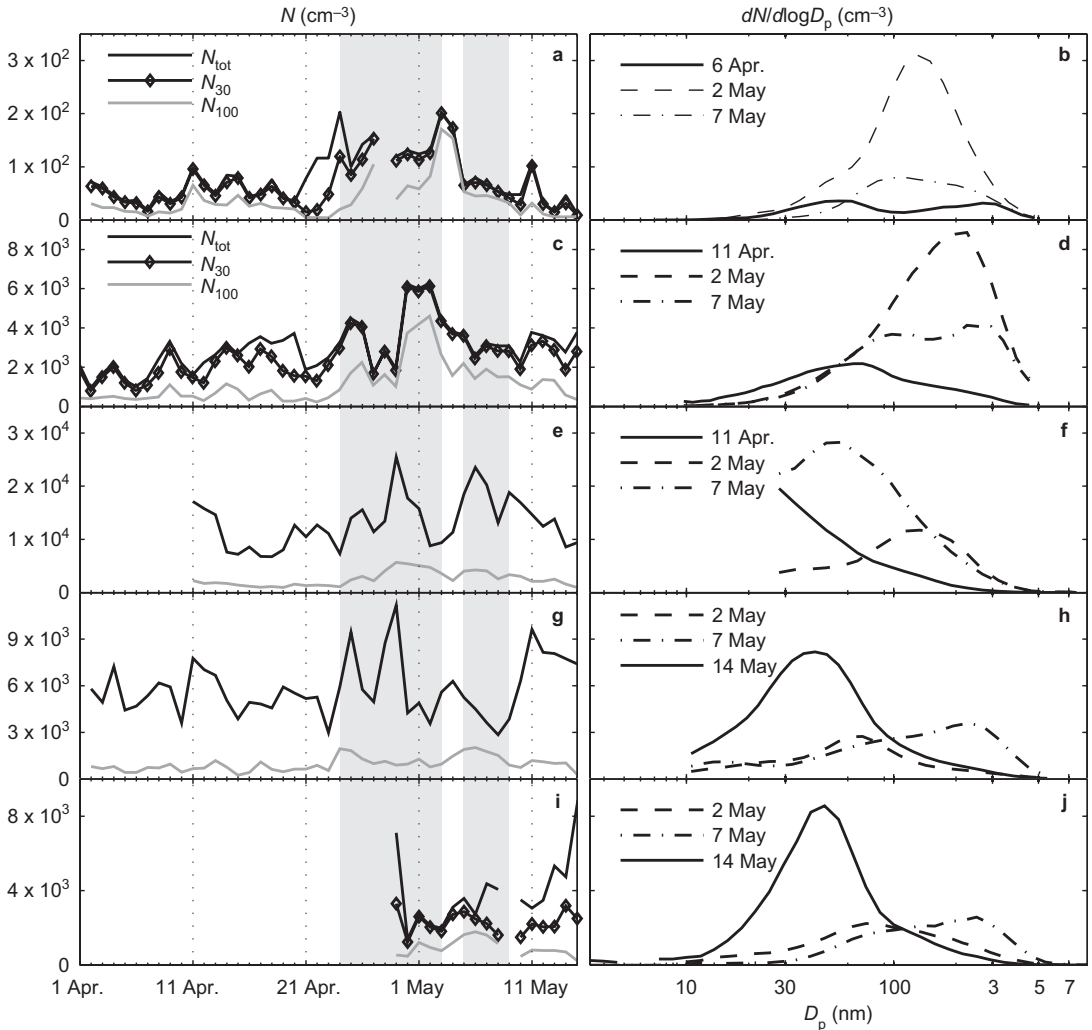
Fig. 6. Left-hand-side panels: Daily mean time series of N_{tot}, N_{100} and N_{30} in diameter at (**a**) Pallas, (**c**) Aspvreten, (**e**) Hornsgatan, (**g**) Malmö and (**i**) Vavihill. The shaded areas delimit POLL1 and POLL2 periods. Right-hand-side panels: Average particle number size distributions on selected dates at (**b**) Pallas, (**d**) Aspvreten, (**f**) Hornsgatan, (**h**) Malmö and (**j**) Vavihill. In **d** and **f**, measurements conducted on 11 April, 2 May and 7 May were taken as representative of REF, POLL1 and POLL2 periods, respectively.

was caused by the smoke plume that shrouded northern Scandinavia on 2 and 7 May, as shown by the model forecasts from the NAAPS Navy Aerosol Analysis and Prediction System model (http://www.nrlmry.navy.mil/aerosol_web/ globaer/ops_01/europe/200605/2006050200_ globaer_ops_europe.gif lower right, and http:// www.nrlmry.navy.mil/aerosol_web/globaer/ ops_01/europe/200605/2006050700_globaer_ ops_europe.gif lower right).

At Aspvreten, mean N_{tot} during the REF period was about 2400 cm^{-3} with a peak number

concentration at 60 nm particle diameter (Fig. 6d). These are typical values for this season at Avspvreten where most air masses trajectories travel over relatively clean areas such as the Arctic and North Atlantic (Tunved *et al.* 2003). During POLL1, mean N_{tot} increased remarkably, reaching a maximum value of about 6500 cm^{-3}. This period was characterised by a high number concentration of accumulation mode particles, as depicted by the N_{100} time series and the particle number size distribution on 2 May, changing the peak mean diameter from 60 nm to 180 nm.
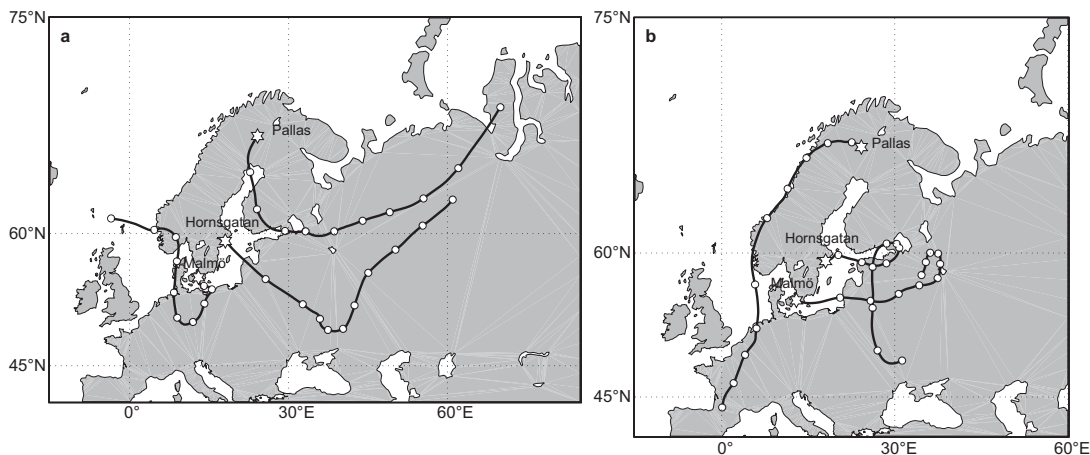
Fig. 7. Five-day backtrajectories arriving at Pallas, Hornsgatan, and Malmö at 00:00 UTC on (**a**) 2 May and (**b**) 7 May 2006 for starting heights of 500 m. White dots are plotted every 12 hours and white stars show the arrival location. The trajectories are plotted on Mercator projection.

The air mass arriving at Aspvreten on 2 May and 7 May at 00:00 UTC passed over the region of wildfires five days prior to its arrival, transporting biomass-burning pollutants to the site (Fig. 7a and b, respectively). N_{100} concentrations increased during the LRT pollution events and a peak appeared in the accumulation mode at about 150 nm in diameter during POLL1 (Fig. 6d). During POLL2, the aerosol number size distribution was bimodal, with peaks at particle diameters of about 100 and 250 nm.

At Hornsgatan, particle number size distributions peaked at diameters smaller than 30 nm (Fig. 6f) on 11 April, before the pollution episodes. According to Gidhagen *et al*. (2004) the peak concentration at this site occurs at about 20 nm, however due to the DMPS cut-off we could not observe this mode in our measurements. To filter out the contribution from traffic emissions at Hornsgatan and to contrast particle number size distributions of the REF, POLL1 and POLL2 periods, we considered only DMPS scans measured between 00:00 and 04:00 LT on weekdays.

As shown by O_3 and PM_{10} time series, the agricultural fire smoke was registered in southern Sweden only during POLL2. On 2 May, the plume stretched from southern Russia and the Ukraine to northern Scandinavia (*see* http://www.nrlmry.navy.mil/aerosol_web/globaer/ops_01/europe/200605/2006050200_globaer_

ops_europe.gif lowr right). Malmö and Vavihill in southern Sweden, however, were unaffected since air masses arriving in this area on that day travelled over the North Atlantic and Germany, not crossing the area of burning fields (Fig. 7a). During POLL2, the smoke plume moved southward, covering southern Sweden (http://www.nrlmry.navy.mil/aerosol_web/globaer/ops_01/europe/200605/2006050700_globaer_ops_europe.gif lower right). The shapes of the aerosol number size distributions at both sites were similar, with a tendency towards elevated accumulation mode particles peaking at 250 nm in diameter (Fig. 6h and j), following the same pattern observed at other stations during the pollution periods.

The average particle number size distributions for Malmö were calculated using scans between 00:00 and 04:00 LT, which were believed to present low influence from local traffic emissions. Because there was no DMPS data for Vavihill during the REF period, we chose 14 May (after POLL2) as the reference day for background conditions. On this day, aerosol number size distributions were deprived of accumulation aerosol and the mode changed to smaller particle diameters (60 nm). The particle number concentrations for both sites were high, reaching about 8000 counts cm^{-3}. Even though the 5-day backtrajectory originated over the Arctic and travelled unperturbed along the

Norwegian coast prior to its arrival at Malmö on 14 May (not shown here), the approach was made from northwest. Wind blowing from this direction typically transports aerosols emitted in and around Malmö's harbour, which is usually associated with ship plumes causing an increase in particle number concentration combined with a modal change to smaller sizes Roldin *et al.* (2011). To quantify the impact of the pollution outbreaks on particle number concentrations, we segregated the data for each station into three particle diameter ranges, Aitken: 30–100 nm (N_{30-100}), accumulation: 100–450 nm ($N_{100-450}$), and 30–450 nm (N_{30-450}). We selected size ranges coincident for all DMPS devices used in this study in order to have a common base on which the comparison could be carried out. Size bin spans were trimmed and only concentrations within coincident intervals were used for integration between 00:00 and 04:00 LT. The cut-off intervals for the integration of N_{30-450} were: Pallas (30–479 nm), Aspvreten (28–451 nm), Hornsgatan (28–453 nm), Vavihill (29–464 nm), and Malmö (28–455 nm). Pallas, Aspvreten and Hornsgatan experienced an increase in

N_{30-450} concentration of 157%, 85% and 39%, respectively (Table 5). However, the figures are much larger when we look at the accumulation mode fraction only. Hornsgatan, whose particle number size distribution is usually dominated by traffic emissions with a modal diameter smaller than 20 nm (Gidhagen *et al.* 2004), experienced an increase of about 200% in the $N_{100-450}$ fraction. Concentrations of N_{30-100} particles for Vavihill and Malmö actually decreased during POLL2, but the change in the accumulation mode size range represented an increase of about 36% for Malmö and 135% for Vavihill. Niemi *et al.* (2010) also found that the particle number concentration increased on average by a factor of 1.8 in the accumulation mode and decreased by a factor of 0.5 in the Aitken and nucleation modes in Hyytiälä during wildfire episodes in Eastern Europe. They hypothesized that the reduction of the smallest particles was caused by suppressed new particle formation due to vapour and molecular cluster uptake by smoke particles.

Summary and conclusions

A suite of air pollution indicators were analysed to assess the impact of spring 2006 transboundary agricultural smoke on the air quality across Sweden. Backward air trajectories and dispersion model results indicated that wildfire emissions were transported from eastern Europe to Scandinavia, where the stations in the northern and central parts of Sweden were subjected to two pollution pulses, and the stations in the south, to one pulse only. The pollution signal around Stockholm was detected with different intensities across the area. Whilst the background stations showed nearly a five-fold increase in PM_{10} concentrations as compared with the non-episode conditions (34 μg m^{-3} against 8 μg m^{-3} at Aspvreten), the signal at the urban stations was not that clear (69 μg m^{-3} against 59 μg m^{-3} at Stockholm's Sveavägen), which suggests that PM_{10} by itself is not a good indicator to flag this sort of events in urban environments. $PM_{2.5}$ concentrations, on the other hand, raised remarkably at all sites, and three- to five-fold increases were measured at the stations across the country irrespective of the station type, i.e. urban or rural

Table 5. Mean particle number concentrations segregated by study periods and size ranges. Numbers in brackets are percentages of particle number concentrations change during the POLL periods as compared with the REF period.

Station	N_{30-100} (cm^{-3})	$N_{100-450}$ (cm^{-3})	N_{30-450} (cm^{-3})
Pallas			
REF	30	20	50
POLL1	76 [151]	52 [165]	128 [157]
POLL2	39 [29]	34 [72]	73 [46]
Aspvreten			
REF	1663	596	2260
POLL1	1578 [–5]	2597 [336]	4175 [85]
POLL2	1533 [–8]	1050 [76]	2584 [14]
Stockholm (Hornsgatan)			
REF	6846	1156	8002
POLL1	7570 [11]	3555 [207]	11125 [39]
POLL2	8451 [23]	2502 [116]	10954 [37]
Vavihill			
REF	2066	693	2759
POLL2	752 [–64]	1625 [135]	2387 [–13]
Malmö			
REF	2742	895	3637
POLL2	2511 [–8]	1220 [36]	3731 [3]

(31 μg m^{-3} against 11 μg m^{-3} at Stockholm's Norrlandsgatan, and 20 μg m^{-3} against 5 μg m^{-3} at Vavihill). These results are in agreement with previous studies that showed that PM$_{2.5}$ concentration is commonly low in the Nordic countries with occasional increases due to biomass burning. At most stations, aerosol number size distributions during the smoke episodes were characterised by a decrease in the Aitken mode particles and a prominent increase in the accumulation mode, resulting in a concentration rise of the latter from 40% at an urban site (Malmö) to 340% at a rural site (Aspvreten) when compared with the clean reference period. Both EC and OC levels increased, with OC making a greater contribution to the total carbonaceous concentrations during the biomass burning episodes. Regardless of the station type, EC/OC ratios decreased at all sites during the pollution periods (between 0.06 and 0.12) as compared with those of the reference period (between 0.18 and 0.27).

Besides particulate matter, the fires also boosted ground-level ozone, raising concentrations of this pollutant by up to 100% at the background stations, thus exceeding national air quality standards. In this aspect, long-range transport can have a considerable impact on PM and gas concentrations in areas with low local emissions and can aggravate air quality conditions in urban conglomerates.

Since climate change predictions indicate a possible increase in the occurrence of dry heat waves in many parts of the globe, these regions will be more susceptible to wildfire episodes. Enforcing changes in current agricultural burning practices is important to avoid air quality deterioration and reduce health impacts in regions close and far downwind of the fires.

References

Andreae M.O. & Merlet P. 2001. Emission of trace gases and aerosols from biomass burning. *Global Biogeochem Cy.* 15: 955–966.

Anttila P., Makkonen U., Hellén H., Kyllönen K., Leppänen S., Saari H. & Hakola H. 2008. Impact of the open biomass fires in spring and summer of 2006 on the chemical composition of background air in south-eastern Finland. *Atmos. Environ.* 42: 6472–6486.

Areskoug H. 2007. *Bestämning av PM$_{10}$ — en jämförelse av de vanligaste mätmetoderna använda i Sverige och den europeiska referensmetoden*. ITM report 168, Stockholm University.

Birch M.E. & Cary R.A. 1996. Elemental carbon-based method for monitoring occupational exposures to particulate diesel exhaust. *Aerosol Sci. Tech.* 25: 221–241.

Boman B.C., Forsberg A.B. & Järvholm B.G. 2003. Adverse health effects from ambient air pollution in relation to residential wood combustion in modern society. *Scand. J. Work Env. Health* 29: 251–260.

Damoah R., Spichtinger N., Forster C., James P., Mattis I., Wandinger U., Beirle S. & Stohl A. 2004. Around the world in 17 days — hemispheric-scale transport of forest fire smoke from Russia in May 2003. *Atmos. Chem. Phys.* 4: 1311–1321.

Draxler R.R. & Rolph G.D. 2011. *HYSPLIT — HYbrid Single-Particle Lagrangian Integrated Trajectory Model*. NOAA Air Resources Laboratory, Silver Spring, MD, available at http://ready.arl.noaa.gov/HYSPLIT.php.

Forsberg B., Hansson H.C., Johansson C., Areskoug H., Persson K. & Järvholm B. 2005. Comparative health impact assessment of local and regional particulate air pollutants in Scandinavia. *Ambio* 34: 11–19.

Frey A.K., Tissari J., Saarnio K.M., Timonen H., Tolonen-Kivimaki O., Aurela M.A., Saarikoski S.K., Makkonen U., Hytönen K., Jokiniemi J., Salonen R.O. & Hillamo R.E.J. 2009. Chemical composition and mass size distribution of fine particulate matter emitted by a small masonry heater. *Boreal Env. Res.* 14: 255–271.

Gidhagen L., Johansson C., Omstedt G., Langner J. & Olivares G. 2004. Model simulations of NOx and ultrafine particles close to a Swedish highway. *Environ. Sci. Technol.* 38: 6730–6740.

Haywood J.M. & Boucher O. 2000. Estimates of the direct and indirect radiative forcing due to tropospheric aerosols: a review. *Rev. Geophys.* 38: 513–543.

ISO 9835 1993. Methods for measurement of air pollution — part 11: determination of a Black Smoke index in ambient air.

Johansson C., Burman L. & Forsberg B. 2009. The effects of congestions tax on air quality and health. *Atmos. Environ.* 43: 4843–4854.

JRC-IES 2007. Forest fires in Europe, Institute for Environ-

ment and Sustainability Report no. 7. Land management and natural hazards unit, European Communities.

Kaufmann Y.J., Tanré D. & Boucher O. 2002. A satellite view of aerosols in the climate system. *Nature* 419: 215–223.

Khalil M.A.K. & Rasmussen R.A. 2003. Tracers of wood smoke. *Atmos. Environ.* 37: 1211–1222.

Krecl P., Targino A.C. & Johansson C. 2011. Spatiotemporal distribution of light-absorbing carbon and its relationship to other atmospheric pollutants in Stockholm. *Atmos. Chem. Phys.* 11: 11553–11567.

Lighty J.S., Veranth J.M. & Sarofim A.F. 2000. Combustion aerosols: factors governing their size and composition and implications to human health. *J. Air Waste Manage.* 50: 1565–1618.

Lin C.I., Baker M.B. & Charlson R.J. 1973. Absorption coefficient of the atmospheric aerosol: a method for measurement. *Appl. Opt.* 12: 1356–1363.

Löndahl J., Pagels J., Massling A., Boman C., Swietlicki E., Rissler J., Blomberg A. & Sandström T. 2008. Deposition of biomass combustion aerosol particles in the human respiratory tract. *Inhal. Toxicol.* 20: 923–933.

Niemi J.V., Tervahattu H., Vehkamäki H., Kulmala M., Koskentalo T., Sillanpää M. & Rantamäki M. 2004. Characterization and source identification of a fine particle episode in Finland. *Atmos. Environ.* 38: 5003–5012.

Niemi J.V., Tervahattu H., Vehkamäki H., Martikainen J., Laakso L., Kulmala M., Aarnio P., Koskentalo T., Sillanpää M. & Makkonen U. 2005. Characterisation of aerosol particle episodes in Finland caused by wild-fires in eastern Europe. *Atmos. Chem. Phys.* 5: 2299–2310.

Norman M. & Johansson C. 2006. Studies of some measures to reduce road dust emissions from paved roads in Scandinavia. *Atmos. Environ.* 40: 6154–6164.

Pio C., Cerqueira M., Harrison R.M., Nunes T., Mirante F., Alves C., Oliveira C., Sanchez de la Campa A., Artíñano B. & Matos M. 2011. OC/EC ratio observations in Europe: re-thinking the approach for apportionment between primary and secondary organic carbon. *Atmos. Environ.* 45: 6121–6132.

Pope A., Burnett R., Thun M., Calle E., Krewski D., Ito K. & Thurston G. 2002. Lung cancer, cardopulmonary mortality, and long-term exposure to fine particulate air pollution. *J. Am. Med. Assoc.* 287: 1132–1141.

Putaud J.-P., Van Dingenen R., Alastuey A., Bauer H., Birmili W., Cyrys J., Flentje H., Fuzzi S., Gehrig R., Hansson H.C., Harrison R.M., Herrmann H., Hitzenberger R., Huglin C., Jones A.M., Kasper-Giebl A., Kiss G., Kousa A., Kuhlbusch T.A.J., Loschau G., Maenhaut W., Molnar A., Moreno T., Pekkanen J., Perrino C., Pitz M., Puxbaum H., Querol X., Rodriguez S., Salma I., Schwarz J., Smolik J., Schneider J., Spindler G., ten Brink H., Tursic J., Viana M., Wiedensohler A. & Raes F. 2010. A European aerosol phenomenology — 3: Physical and chemical characteristics of particulate matter from 60 rural, urban, and kerbside sites across Europe. *Atmos. Environ.* 44: 1308–1320.

Reid J.S., Koppmann R., Eck T.F. & Eleuterio D.P. 2005. A review of biomass burning emissions part II: intensive physical properties of biomass burning particles. *Atmos. Chem. Phys.* 5: 799–825.

Roldin P., Swietlicki E., Massling A., Kristensson A., Löndahl J., Eriksson A., Pagels J. & Gustafsson S. 2011. Aerosol ageing in an urban plume — implications for climate. *Atmos. Chem. Phys.* 11: 5897–5915.

Saarikoski S., Sillanpää M., Sofiev M., Timonen H., Saarnio K., Teinilä K., Karppinen A., Kukkonen J. & Hillamo R. 2007. Chemical composition of aerosols during a major biomass burning episode over northern Europe in spring 2006: Experimental and modelling assessments. *Atmos. Environ.* 41: 3577–3589.

Sillanpää M., Frey A., Hillamo R., Pennanen A., Spolnik Z., van Grieken R., Sandell E., Pennanen A.S. & Salonen R.O. 2005. Organic, elemental and inorganic carbon in particulate matter of six urban environments in Europe. *Atmos. Chem. Phys.* 5: 2869–2879.

Sopauskiene D. & Jasineviciene D. 2009. Variations of concentration of aerosol particles (< 10 μm) in Vilnius. *Lith. J. Phys.* 49: 323–334.

Stohl A., Berg T., Burkhart J.F., Fjæraa A.M., Forster C., Herber A., Hov Ø., Lunder C., McMillan W.W., Oltmans S., Shiobara M., Simpson D., Solberg S., Stebel K., Ström J., Tørseth K., Treffeisen R., Virkkunen K. & Yttri K.E. 2007. Arctic smoke — record high air pollution levels in the European Arctic due to agricultural fires in eastern Europe in spring 2006. *Atmos. Chem. Phys.* 7: 511–534.

Treffeisen R., Tunved P., Ström J., Herber A., Bareiss J., Helbig A., Stone R.S., Hoyningen-Huene W., Krejci R., Stohl A. & Neuber R. 2007. Arctic smoke-aerosol characteristics during a record smoke event in the European Arctic and its radiative impact. *Atmos. Chem. Phys.* 7: 3035–3053.

Tunved P., Hansson H.C., Kulmala M., Aalto P., Viisanen Y., Karlsson K., Kristensson A., Swietlicki E., Dal Maso M., Ström J. & Komppula M. 2003. One year boundary layer aerosol size distribution data from five Nordic background stations. *Atmos. Chem. Phys.* 3: 2183–2205.

Ulevicius V., Bycenkiene S., Spirkauskaite N. & Kecorius S. 2010. Biomass burning impact on black carbon aerosol mass concentration at a coastal site: case studies. *Lith. J. Phys.* 50: 335–344.

WHO 2006. *Air quality guidelines global update 2005*. World Health Organization Regional Office for Europe, Copenhagen.

Witham C. & Manning A. 2007. Impacts of Russian biomass burning on UK air quality. *Atmos. Environ.* 41: 8075–8090.